

CHARACTERIZING SECONDARY SHOCK EFFECTS IN OLIVINE FROM A POTENTIAL MANTLE-DERIVED DUNITE CLAST WITHIN LUNAR METEORITE NORTHWEST AFRICA (NWA) 14900 USING ELECTRON BACKSCATTER DIFFRACTION (EBSD) D. Sheikh¹ and A. M. Ruzicka¹, ¹Cascadia Meteorite Laboratory, Portland State University, Department of Geology, Portland, OR 97239, USA (dsheikh@pdx.edu).

Introduction: The ongoing search for potential mantle-derived rocks (e.g., dunites, harzburgites) from the Moon is critical for advancing our knowledge to better understand the evolution of the lunar interior and the lithologies that comprise it [1]. Previously, we examined a 2.2 mm dunite clast from lunar meteorite Northwest Africa (NWA) 14900 [2] and suggested that it could represent a fragment of the lunar mantle based on its relatively primitive mineralogy (99.2 area % olivine, 0.8 area % chromite) and mineral compositions (olivine Mg# = 91.0±0.1; chromite Mg# = 51.3±1.0, Cr# = 79.3±0.3) compared to other hypothesized mantle-derived dunites [3-4]. However, unlike other candidate lunar mantle dunites, which generally contain either additional mineral phases (e.g., pyroxene + plagioclase) [3] or symplectites (e.g., Cr-spinel + pyroxene) [4] that can provide important constraints on equilibrium pressures within the lunar interior (which can be converted into equilibrium depths), the essentially monomineralic nature of the NWA 14900 dunite clast requires an alternative approach to potentially evaluate a lunar mantle origin for this dunite clast. Although one may assume that the calculated equilibrium temperature of the dunite clast ($T_{\text{equil}} = 967 \pm 11$ °C) obtained using the olivine-spinel Fe-Mg geothermometer [5] can be plotted onto existing modeled selenotherms [6] to potentially infer an equilibrium depth, the role of impacts on both physically and chemically modifying lunar materials needs to be properly evaluated in order to disentangle secondary shock effects [7] within the dunite clast, as post shock heating can result in a lower T_{equil} due to sub-solidus re-equilibration. Here, we investigate olivine grains from the dunite clast using electron backscatter diffraction [EBSD] methods [8-10] to constrain the shock deformation history of the clast, with the goal of evaluating whether it represents a fragment of the lunar mantle, or an Mg-suite dunite [11].

Results: Phases identified within the dunite clast by EBSD include olivine (comprises ~99.9 % of pixels) and chromite (~0.1 %), which is consistent with the estimated mineral modal abundances for the dunite clast using EDS chemical mapping [2], indicating correct phase indexing. Below, based on the olivine inverse pole figure (IPF_x) orientation maps, we divide the dunite clast into two distinct regions, which we denote as “coarse” and “granular” regions (Fig. 2).

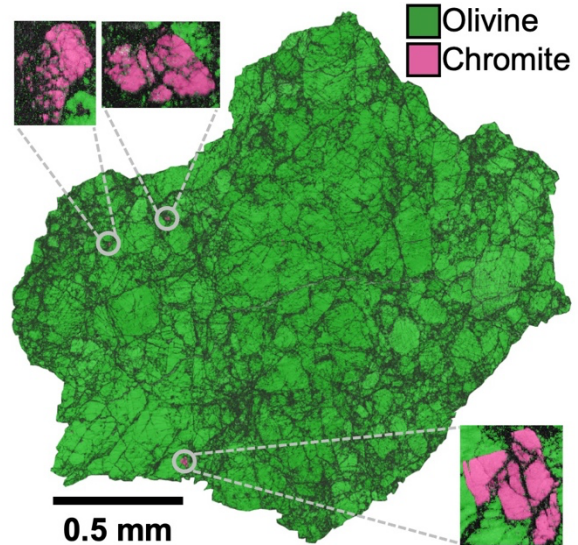


Fig. 1. Phase + band contrast (BC) map of NWA 14900 dunite clast. Zoomed insets display chromite grains.

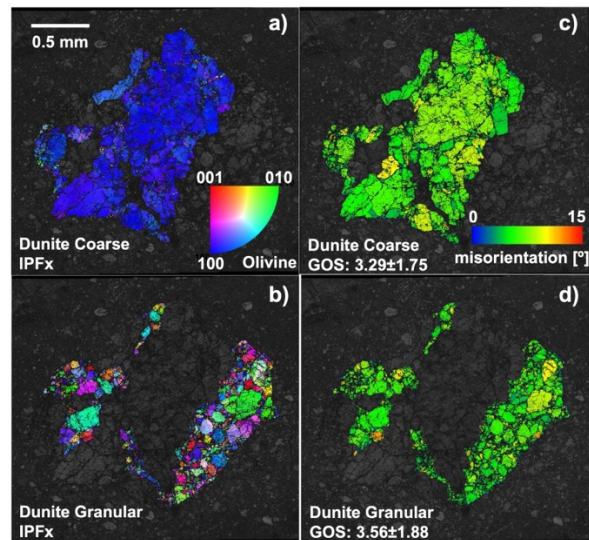


Fig. 2. Inverse pole figure (IPF_x) and grain orientation spread (GOS) maps of coarse (a, c) and granular (b, d) regions of dunite clast, respectively.

Dunite Coarse Region: This region is composed of what could be a single, coarse (≥ 2 mm long), fractured and deformed olivine grain with one dominant orientation that is more variable in the $\langle 010 \rangle$ and $\langle 001 \rangle$ crystal directions than in the $\langle 100 \rangle$ direction (Fig. 2a, 3). This region is heterogeneously deformed (Fig. 2c),

with an average grain orientation spread (“average misorientation within a grain”, GOS) value ($3.29 \pm 1.75^\circ$) consistent with a shock stage between $\sim S3-S4$ [7-8]. From the olivine crystal rotation axis (CRA) plot, low angle ($2-10^\circ$) grain boundaries within the coarse region are primarily misoriented along the $\langle 100 \rangle$ rotation axis (Fig. 4a), consistent with the predominance of c-type slip in olivine [8, 12]; calculation of T_{deform} [8-9] yields a deformation temperature of $856 \pm 93^\circ\text{C}$.

Dunite Granular Region: This region is comprised of olivine grains which do not display any obvious preferred crystal orientation (Fig. 2b). Several grains in the granular region appear to display the same crystallographic orientation as the contiguous olivine grains in the coarse region in IPF_x, which likely represents pieces of the coarse region connected in the third dimension. Like the coarse region, the granular region is also heterogeneously shocked (Fig. 2d) and displays a predominance of c-type slip in olivine (Fig. 4b), however, both the average GOS value ($3.56 \pm 1.88^\circ$) and T_{deform} ($876 \pm 92^\circ\text{C}$) are slightly higher in the granular region.

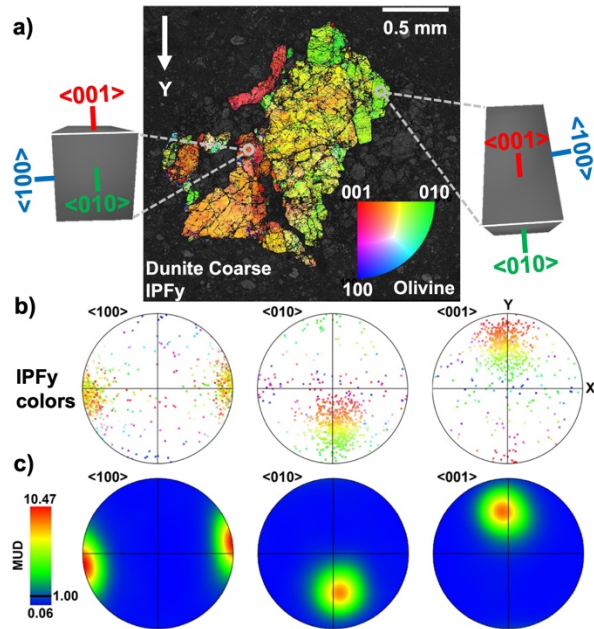


Fig. 3. a) IPF_y map of dunite clast coarse region; rectangular prisms denote unit cell orientations for a given olivine grain orientation within the coarse region. Pole figures of olivine (1 point per grain) from coarse region using (b) IPF_y colors, and (c) contoured colors in terms of multiples of uniform density (MUD) values.

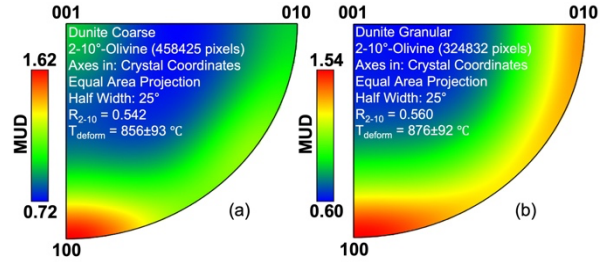


Fig. 4. Crystal rotation axis (CRA) plots for olivine from (a) coarse region, and (b) granular region of dunite clast; plots contoured by color in terms of MUD values.

Discussion: Our interpretation of the history of the dunite clast is as follows: 1) crystallization of a precursor dunite under plutonic conditions, either the upper mantle after lunar magma ocean overturn or an Mg-suite pluton in the lower crust, 2) excavation of the dunite clast from depth by a large basin-forming impactor and emplacement at shallower depth, followed by sub-solidus re-equilibration to T_{equil} to $967 \pm 11^\circ\text{C}$, 3) excavation of the dunite clast to the lunar surface by a second impact event (resulting in brecciation of the coarse region and/or grain boundary sliding to form the granular region, and overprinting of shock deformation resulting in T_{deform} of $856 \pm 93^\circ\text{C}$ and $876 \pm 92^\circ\text{C}$ in the coarse and granular regions, respectively; the slightly higher GOS and T_{deform} in the granular region could have resulted from localized shear heating introduced during brecciation), and 4) incorporation of the dunite clast into NWA 14900 by a third impact event. Alternatively, it is possible that T_{equil} and T_{deform} represent the same event, in which case only one impact event would be responsible for steps 2 and 3. Ongoing work will help to better constrain the link between T_{deform} and T_{equil} , and hopefully help in distinguishing between a crustal or mantle origin.

Acknowledgments: Grant support from the Barringer Crater Company Family Fund for Meteorite Impact Research is gratefully acknowledged.

References: [1] Moriarty D. P. et al. (2021) *Nat. Comm.*, 12, 1-11. [2] Sheikh D. et al. (2022) *MetSoc* 84, abstract #6077. [3] Treiman A. H. and Semprich J. (2023) *AM*, 108, 2182–2192. [4] Bhanot K. K. et al. (2024) *MaPS*, 59, 1-21. [5] Jianping L. et al. (1995) *CJG*, 14, 68-77. [6] Khan A. et al. (2014) *JGR*, 119, 1-25. [7] Stöffler D. et al. (2018) *MaPS*, 53, 5-49. [8] Ruzicka A. M. et al. (2024) *GCA*, 378, 1-35. [9] Ruzicka A. M. and Hugo R. C. (2018) *GCA*, 234, 115-147. [10] Sheikh D. and Ruzicka A. M. (2024) *MetSoc* 86, abstract #6468. [11] Shearer C. K. et al. (2015) *AM*, 100, 294-325. [12] Karato S. et al. (2008) *Annual Rev. Earth Planet. Sci.*, 36, 59-95.